Published in final edited form as:
Eur J Radiol. 2009 May ; 70(2): 305–311. doi:10.1016/j.ejrad.2009.01.053.

Molecular Imaging of Vessels in Mouse Models of Disease

Lyubomir Zagorchev, Ph.D.[1,3] and **Mary J. Mulligan-Kehoe, Ph.D.**[1,2,§]

[1]Angiogenesis Research Center, Dartmouth Medical School, Lebanon, NH

[2]Department of Surgery, Vascular Section, Dartmouth Medical School, Lebanon, NH

[3]Clinical Sites Research Program, Philips Research North America, Briarcliff Manor, NY

Abstract

Vascular imaging of angiogenesis in mouse models of disease requires multi modal imaging hardware capable of targeting both structure and function at different physical scales. The three dimensional (3D) structure and function vascular information allows for accurate differentiation between biological processes. For example, image analysis of vessel development in angiogenesis vs. arteriogenesis enables more accurate detection of biological variation between subjects and more robust and reliable diagnosis of disease. In the recent years a number of micro imaging modalities have emerged in the field as preferred means for this purpose. They provide 3D volumetric data suitable for analysis, quantification, validation, and visualization of results in animal models. This review highlights the capabilities of microCT, ultrasound and microPET for multimodal imaging of angiogenesis and molecular vascular targets in a mouse model of tumor angiogenesis. The basic principles of the imaging modalities are described and experimental results are presented.

Introduction

Angiogenesis is the formation of capillaries from existing vessels[1], which occurs during embryonic development and in adults in either a physiological[2-4] or pathological[5] situation. Formation of angiogenic vessels is regulated by growth factors, integrins, membrane-bound proteinases and the composition of the extracellular matrix (ECM) [6-8]. Each of these factors stimulate extracellular and intracellular signaling cues that work in concert to promote angiogenic processes that regulate endothelial cell branching, sprouting, lumen formation and proliferation[6]. Anti-angiogenic factors are produced during the angiogenic process to maintain the balance of pro-angiogenic molecules and their effects on endothelial cells.

The vascular endothelium is normally maintained in a differentiated, quiescent state. Pro-angiogenic factors destabilize the quiescent endothelium into migratory, proliferative endothelial cells which are attenuated by anti-angiogenic factors. The pro- and anti-angiogenic molecules have cell survival and death functions that are tightly controlled to maintain a balance [8-11].

Many negative regulators of angiogenesis are cleavage products of ECM proteins that are not inhibitory in their normal intact conformation, such as matrix proteins collagen XVIII and IV

§To whom correspondence should be addressed: Mary Jo Mulligan-Kehoe Dartmouth Medical School Borwell 530 E, 1 Medical Center Drive Lebanon, NH 03756 mary.j.mulligan-kehoe@dartmouth.edu Phone: (603) 650-8597 Fax: (603) 650-4928.

and hemostatic proteins such as plasminogen[12-18]. The breakdown of these proteins destabilizes the extracellular matrix, which leads to collapse and regression of capillary tubes. In other cases an extracellular protein may possess angiogenic properties, while its cleavage product is anti-angiogenic. This is the case for plasminogen activator inhibitor-1(PAI-1), which has been shown to be pro-angiogenic [19-21] while a cleaved PAI-1, rPAI-1_{23}, is a potent inhibitor of angiogenesis. In arterial endothelial cells, it inhibits pro-angiogenic fibroblast growth factor-2 (FGF-2) signaling pathways and functions[22, 23]. In mouse models of vascular disease, rPAI-1_{23} inhibits angiogenic vessels to result in reduced disease progression.

The complexity of the physiological processes involved in angiogenesis at the cellular level is enormous. In many cases a single imaging modality can not provide enough details and information about the underlined interactions. For example, functional imaging modalities lack information about structure. It is impossible to determine the size of vessels from imaging modalities such as SPECT and PET or ultrasound. A multimodal imaging approach where functional information acquired from molecular imaging modalities is complemented with structural details is often required for successful imaging studies and verification of results.

Like normal tissue, tumors require nutrients in order to grow and survive. The neo-vasculature of tumors provides a means of supplying oxygen and nutrients to the tumor once it reaches a certain size. The tumor cells secrete specific molecules that promote recruitment of host vessels to the tumor, a process called angiogenesis. The very subtle stage of tumor induced angiogenesis is now the primary focus of study in the vascular biology field. The following sections review our modalities of choice for vascular imaging of models of disease implanted in mice; describe their current state, and present examples of their application for imaging of angiogenesis.

MicroPET, microCT, ultrasound and confocal imaging have become valuable tools for studying the tumor vasculature in small animal models. Each of these modalities provides unique advantages over the other. This review will discuss each in the context of tumor angiogenesis with emphasis on distinct advantages and disadvantages each brings to the imaging field.

IMAGING MODALITIES

MicroCT

Micro Computed Tomography (MicroCT) is a structural imaging modality that provides differentiation of contrast-enhanced tissues or structures with high attenuation from non-enhanced soft tissues[24, 25]. Traditional MicroCT imaging applications include screening for anatomical abnormalities[26-31] as well as detection and quantification of changes in live animals[32, 33] or tissue samples removed from sacrificed animals[34]. Most current *in vivo* MicroCT scanners have resolutions ranging from 100 to 30 μm, while *ex vivo* scanners have resolutions from 30 to 1 μm. The imaging is a two-step procedure. In the first step, 2D X-ray projections of the imaged object at different orientations of the x-ray source or object are acquired by the x-ray detector. In the second step the acquired projections are first corrected for various image artifacts and/or distortions due to sensor nonlinearity and then used to reconstruct the final volumetric data representing the scanned object in 3D. Depending on the parameters of the imaging protocol, a scan may take from several minutes to hours. During image acquisition, X-rays emitted by the source are attenuated as they pass through the imaged object. This proportionally reduces the original intensity of the X-rays due to absorption or scatter of photons[24, 25]. Objects with low attenuation properties, like soft tissue, allow most of the X-rays to pass through the object unabsorbed and arrive at the detector on the other end. However, if the imaged object has high attenuating properties, such as bone for example, fewer X-rays will have the kinetic energy to arrive at the detector.

In molecular imaging of vessels in mouse models of disease, we are interested in the vascular structures whose attenuation properties differ very little from the surrounding soft tissue. Consequently, vascular MicroCT requires the use of contrast agents such as Fenestra, Microfil, and Bismuth. The contrast agents either circulate in the blood pool or are used to replace it. An example of a three-dimensional (3D) MicroCT volume showing the vasculature of a tumor sample is shown in Figure 1 below.

MicroCT has emerged as an important structural imaging modality for vascular applications and angiogenesis due to its high spatial resolution[34]. It provides a high resolution 3D representation of vascular structures that directly reflects the level of angiogenesis or inhibition/development of neo-vasculature and provides a quantitative means for assessment of tumor growth over time. MicroCT data can be used to obtain measures such as vascular volume, tumor volume[35], vascular surface area[36], vessel density[37], and branching patterns[38, 39] which can be then combined/fused with functional information available from molecular imaging techniques such as PET, SPECT, MRI, or Ultrasound. Volume rendering showing the neo-vasculature and volume of tumors can be obtained from the microCT images, as demonstrated in Figure 2 which compares the vasculature of mice treated with saline or the angiogenesis inhibitor, rPAI-1_{23}.

Ultrasound

Ultrasound is another modality for imaging of angiogenesis in vivo[24, 25, 40]. A transmitter produces s train of short pulses of high frequency oscillations, which are transformed by a transducer into high frequency mechanical oscillations. The vibrational energy of the mechanical oscillations is directed into the scanned object and swept back and forth. The return of an echo depends mainly on the type of scanned object/tissue and penetration depth. Echoes are detected by the transducer and transformed into electrical signals that are processed by a receiver to create an image.

High frequency micro-ultrasound imaging[41] is particularly useful for obtaining repeated, non-invasive in vivo measurements to assess growth and to insure tumors are at the same size at initiation of treatment. In-vivo microCT has a limited application for tumor measurements because of the typically lower resolution of in-vivo scanners i.e. 50 microns. In addition, it gives a significant dose of radiation to the animal that may interfere with the study. Ex-vivo microCT has a much higher resolution, but requires samples from sacrificed animals. Therefore, it is not possible to image the same animal over time. Unlike microCT, ultrasound is non invasive, does not interfere with the study by using radiation and can be utilized to measure tumor size and volume repeatedly. Such measurements are important for every study in order to determine animals with relatively similar tumor measurements, which can be then divided into groups. MRI can be used to measure tumor volume but in most cases it is cost prohibitive comparing to ultrasound.

Other applications of ultrasound include spectral and power doppler ultrasounds[42-44] used to measure blood flow velocities. Ultrasound contrast agents for angiogenesis have also been developed[45]. They are gas-filled microbubbles that are administered intravenously to the systemic circulation. Their size is in the range of 1 to 5 μm, which allows circulation in the capillary network. Microbubbles are strongly echogenic due to their large acoustic impedance mismatch with the surroundings. The response of an ultrasound contrast agent to an acoustic field depends on the applied mechanical index, which is proportional to the peak pressure of the acoustic wave divided by the square root of its frequency. At a low mechanical index (MI<0.1), the particles show Rayleigh scattering of the impinging wave, which increases with the sixth power of the particle radius and is dampened with increasing shell stiffness and gas density of the interior phase. At intermediate mechanical index (0.1<MI<0.5), microbubbles start to resonate in the sound field, producing also higher harmonics, which can be exploited

using higher harmonic imaging. Increasing the mechanical index further (i.e. MI>0.5) also allows to disrupt the agents and release the trapped interior phase. That event produces not only a strong characteristic signal, but can also be used for therapeutic application, such as drug delivery.

Microbubbles can be used to image blood perfusion in organs and measure blood flow rate in the heart, in tumors, or other organs[46]. Targeted ligands that bind to specific receptors expressed on the vascular endothelium can be conjugated to microbubbles, enabling the microbubble complex to accumulate selectively in areas of interest, such as neo-vasculature or diseased/abnormal tissues. That form of molecular imaging is known as targeted contrast-enhanced ultrasound. It generates a strong signal if the targeted microbubbles bind to the receptors expressed on the area of interest. Furthermore, targeted contrast-enhanced ultrasound has many other applications in both delivery of therapeutics and medical diagnostics. The inhibition of tumor angiogenesis induced by rPAI-1_{23} and imaged with ultrasound is shown in Figure 3.

MicroPET

Micro positron emission tomography (microPET) is another imaging modality that allows for visualization and quantitative assessment of angiogenesis in vivo[47-49]. MicroPET provides 3D image volumes representing the temporal and spatial distribution of a contrast agent (radioisotope) localized at a target[50]. The radioactive agent decays by positron emission. A positron travels a very short distance in tissue (<2mm) before colliding with an ordinary atomic electron. The two annihilate and a pair of high energy photons comes into existence. The photons travel in opposite directions at the speed of light. Detection of many such pairs leads to localization of their origin and ultimately, the creation of an image[24, 25].

The main advantage of microPET over other imaging modalities is its high sensitivity. Very low concentrations of a radioisotope are sufficient to delineate a lesion based on its physiological characteristics. Furthermore, because there is limited background radiation, microPET inherently has a high signal to noise ratio. Due to the small size of the label (a radioactive atom *vs*. a microbubble 2-6μm) the contrast agent is readily available in the capillary network and can be used in combination with any other type of targeting agents such as metabolic substrates, small organic molecules, peptides, macromolecules, antibodies, nanoparticles, microbubbles, etc., to image any type of target.

Kinetic models are often used to describe the dynamics involved in the utilization of the radioisotopes[51-54]. The models consist of compartments and attempt to capture the spatial and temporal distributions of the isotopes that result from the complex physiological events at the cellular level. They are aimed at understanding and quantifying the physiological interactions of the radioactively labeled compound in a particular micro-environment. The resulting kinetic models describe the tracer behavior and provide a means for quantitative analysis of microPET data.

Recently antibody targeting of receptors for angiogenic growth factors[55-57] and integrins associated with angiogenesis[58-60] have received considerable attention as potential therapeutics in the treatment of cancer. The added advantage of antibody therapy is that the antibody can be conjugated to a radioactive molecule for imaging of the tumor vasculature. MicroPET has become a favorite imaging modality for antibody targeted imaging and therapy. In many cases copper-64 (Cu-64) is the preferred isotope due to its longer half life (12.7h)[61, 62] and reduced background[53].

One scheme for imaging angiogenesis is to Cu-64 label an antibody specific for an epitope on vascular endothelial growth factor receptor-2 (VEGFR-2), which is expressed on angiogenic vessels. The labeled antibody is administering by intravenous injection into the vasculature of

a tumor-bearing mouse as illustrated in Figure 4. Kinetic modeling of the acquired microPET data can be used to determine the concentration of antigen-bound antibody in the tumor vasculature and provide a sense of the expression level of the imaging target as well as wash in/out rates[51, 63, 64].

Confocal Microscopy

Confocal microscopy is one approach to optical molecular imaging that provides reconstruction of 3D images. In this technique, serial optical sections can be collected from specimens thereby allowing reconstruction of their third dimension by stacking the images on top of each other (commonly referred to as z-stacks). It is not a medical imaging modality as the ones described above, but employs targeted molecular imaging of specific biological molecules[65-67]. Targeted molecules are probed by using a fluorophore-tagged antibody specific for vascular targets found on endothelial or smooth muscle cells. Another alternative is using two sets of antibodies: primary and secondary. The primary antibody probes the target of interest, while a fluorophore-labeled secondary antibody amplifies the interaction of the primary antibody with the target molecule. The advantage of this technique is that the signal can be amplified and co-localized molecules can be detected through the use of secondary antibodies labeled with different fluophores that can be detected at different wave lengths. This technique can be applied to cultured cells or tissue sections.

Confocal microscopy plays a very important role in correlation and validation of results. In vascular imaging experiments collected Z-stacks can be thresholded to segment out the signal of the fluorophore bound to the specific target expressed on the blood vessel. Given the total volume of the z-stack, $\boldsymbol{V_Z}$, and the volume of the bound stain, $\boldsymbol{V}$s, the density of the imaged target can be measured as the ratio of the volume of the bound stain over the volume of the stack: $\boldsymbol{V_S/V_Z}$. This is illustrated in Figure 5.

Fusion of Multimodal Data

Functional imaging modalities such as microPET reveal valuable insights into biochemical, physiological, and pharmacological processes in vivo. Their major limitation, however, is the lack of high spatial resolution and detailed anatomical or vascular information. This problem can be easily alleviated by using complementary information provided by a structural imaging modality such as microCT and techniques from image registration.

Image registration can be rigid or nonrigid. Rigid registration deals with the alignment of rigid objects or objects that can not change shape or deform locally, such as bone fragments. Nonrigid registration, on the other hand, deals with the alignment of volumes of deformable or nonrigid objects and is very important for vascular analysis of mouse models of disease. Many algorithms for both rigid and nonrigid registration have been developed[68-70]. The accuracy of any algorithm for image registration can be quantified as the difference between true and estimated positions of all image points. The smaller the difference, the more accurate the registration, but determining the position of the same point in two volumes of a nonrigid object may not always be an easy task[71]. Unless a point is unique and can be detected in the two volumes, such a measure can not be computed because an image point from one volume may not exist in another. Despite such difficulties, as illustrated in Figure 6, functional activity from microPET can be overlaid with structural information from microCT for more detailed analysis and validation of results.

CONCLUSION

The field of angiogenesis is a rapidly growing area in which multimodal molecular imaging efforts are transforming the established understanding of the field. Vascular imaging

techniques, as the ones described above, provide a valuable combination of structural and functional information that has the potential to advance the angiogenesis related research. The molecular imaging of vessels in mouse models of disease is extremely important to our understanding of the mechanisms that contribute to the progression of diseases such as cancer and ischemic diseases. Utilization of complimentary information provided by small animal imaging modalities provides the necessary basis for successful analysis and evaluation of imaging studies.

ACKNOWLEDGEMENTS

This study was supported by Dartmouth-Philips Research Consortium (MJM-K).

REFERENCES

1. Folkman J. How is blood vessel growth regulated in normal and neoplastic tissue? G.H.A. Clowes memorial Award lecture. Cancer Res Feb;1986 46(2):467–473. [PubMed: 2416426]
2. Alon T, Hemo I, Itin A, Pe'er J, Stone J, Keshet E. Vascular endothelial growth factor acts as a survival factor for newly formed retinal vessels and has implications for retinopathy of prematurity. Nat Med Oct;1995 1(10):1024–1028. [PubMed: 7489357]
3. Ferrara N. Role of vascular endothelial growth factor in regulation of physiological angiogenesis. Am J Physiol Cell Physiol Jun;2001 280(6):C1358–1366. [PubMed: 11350730]
4. Ferrara N, Chen H, Davis-Smyth T, Gerber HP, Nguyen TN, Peers D, Chisholm V, Hillan KJ, Schwall RH. Vascular endothelial growth factor is essential for corpus luteum angiogenesis. Nat Med Mar; 1998 4(3):336–340. [PubMed: 9500609]
5. Folkman J. Angiogenesis in cancer, vascular, rheumatoid and other disease. Nat Med Jan;1995 1(1): 27–31. [PubMed: 7584949]
6. Davis GE, Bayless KJ, Mavila A. Molecular basis of endothelial cell morphogenesis in three-dimensional extracellular matrices. The Anatomical record Nov 1;2002 268(3):252–275. [PubMed: 12382323]
7. Senger DR. Molecular framework for angiogenesis: a complex web of interactions between extravasated plasma proteins and endothelial cell proteins induced by angiogenic cytokines. The American journal of pathology Jul;1996 149(1):1–7. [PubMed: 8686733]
8. Stupack DG, Cheresh DA. Apoptotic cues from the extracellular matrix: regulators of angiogenesis. Oncogene Dec 8;2003 22(56):9022–9029. [PubMed: 14663480]
9. Folkman J. Fundamental concepts of the angiogenic process. Curr Mol Med Nov;2003 3(7):643–651. [PubMed: 14601638]
10. Folkman J, Klagsbrun M. Angiogenic factors. Science Jan 23;1987 235(4787):442–447. [PubMed: 2432664]
11. Hanahan D, Folkman J. Patterns and emerging mechanisms of the angiogenic switch during tumorigenesis. Cell Aug 9;1996 86(3):353–364. [PubMed: 8756718]
12. Cao Y, Ji RW, Davidson D, Schaller J, Marti D, Sohndel S, McCance SG, O'Reilly MS, Llinas M, Folkman J. Kringle domains of human angiostatin. Characterization of the anti-proliferative activity on endothelial cells. J Biol Chem Nov 15;1996 271(46):29461–29467. [PubMed: 8910613]
13. Colorado PC, Torre A, Kamphaus G, Maeshima Y, Hopfer H, Takahashi K, Volk R, Zamborsky ED, Herman S, Sarkar PK, Ericksen MB, Dhanabal M, Simons M, Post M, Kufe DW, Weichselbaum RR, Sukhatme VP, Kalluri R. Anti-angiogenic cues from vascular basement membrane collagen. Cancer Res May 1;2000 60(9):2520–2526. [PubMed: 10811134]
14. Kamphaus GD, Colorado PC, Panka DJ, Hopfer H, Ramchandran R, Torre A, Maeshima Y, Mier JW, Sukhatme VP, Kalluri R. Canstatin, a novel matrix-derived inhibitor of angiogenesis and tumor growth. J Biol Chem Jan 14;2000 275(2):1209–1215. [PubMed: 10625665]
15. Maeshima Y, Sudhakar A, Lively JC, Ueki K, Kharbanda S, Kahn CR, Sonenberg N, Hynes RO, Kalluri R. Tumstatin, an endothelial cell-specific inhibitor of protein synthesis. Science Jan 4;2002 295(5552):140–143. [PubMed: 11778052]

16. O'Reilly MS, Boehm T, Shing Y, Fukai N, Vasios G, Lane WS, Flynn E, Birkhead JR, Olsen BR, Folkman J. Endostatin: an endogenous inhibitor of angiogenesis and tumor growth. Cell Jan 24;1997 88(2):277–285. [PubMed: 9008168]

17. Sasaki T, Larsson H, Tisi D, Claesson-Welsh L, Hohenester E, Timpl R. Endostatins derived from collagens XV and XVIII differ in structural and binding properties, tissue distribution and anti-angiogenic activity. J Mol Biol Sep 1;2000 301(5):1179–1190. [PubMed: 10966814]

18. Staton CA, Brown NJ, Rodgers GR, Corke KP, Tazzyman S, Underwood JC, Lewis CE. Alphastatin, a 24-amino acid fragment of human fibrinogen, is a potent new inhibitor of activated endothelial cells in vitro and in vivo. Blood Jan 15;2004 103(2):601–606. [PubMed: 14512300]

19. Durand MK, Bodker JS, Christensen A, Dupont DM, Hansen M, Jensen JK, Kjelgaard S, Mathiasen L, Pedersen KE, Skeldal S, Wind T, Andreasen PA. Plasminogen activator inhibitor-I and tumour growth, invasion, and metastasis. Thrombosis and haemostasis Mar;2004 91(3):438–449. [PubMed: 14983218]

20. Lijnen HR. Pleiotropic functions of plasminogen activator inhibitor-1. J Thromb Haemost Jan;2005 3(1):35–45. [PubMed: 15634264]

21. Pepper MS. Role of the matrix metalloproteinase and plasminogen activator-plasmin systems in angiogenesis. Arteriosclerosis, thrombosis, and vascular biology Jul;2001 21(7):1104–1117.

22. Drinane M, Walsh J, Mollmark J, Simons M, Mulligan-Kehoe MJ. The anti-angiogenic activity of rPAI-1(23) inhibits fibroblast growth factor-2 functions. The Journal of biological chemistry Nov 3;2006 281(44):33336–33344. [PubMed: 16950776]

23. Mulligan-Kehoe MJ, Wagner R, Wieland C, Powell R. A truncated plasminogen activator inhibitor-1 protein induces and inhibits angiostatin (kringles 1-3), a plasminogen cleavage product. The Journal of biological chemistry Mar 16;2001 276(11):8588–8596. [PubMed: 11113116]

24. Bushberg, J.; Seibert, J.; Leidholdt, E.; Boone, J. The Essential Physics of Medical Imaging. Vol. 2nd ed. Lippencott, Williams and Wilkins; 2002.

25. Wolbarst, A. Physics of Radiology. Vol. 2nd ed. Medical Physics Publishing; Madison Wisconsin: 2005.

26. Bouxsein ML, Uchiyama T, Rosen CJ, Shultz KL, Donahue LR, Turner CH, Sen S, Churchill GA, Muller R, Beamer WG. Mapping quantitative trait loci for vertebral trabecular bone volume fraction and microarchitecture in mice. J Bone Miner Res Apr;2004 19(4):587–599. [PubMed: 15005846]

27. Engelke K, Karolczak M, Lutz A, Seibert U, Schaller S, Kalender W. Micro-CT. Technology and application for assessing bone structure. Der Radiologe Mar;1999 39(3):203–212. [PubMed: 10218213]

28. Graichen H, Lochmuller EM, Wolf E, Langkabel B, Stammberger T, Haubner M, Renner-Muller I, Englmeier KH, Eckstein F. A non-destructive technique for 3-D microstructural phenotypic characterisation of bones in genetically altered mice: preliminary data in growth hormone transgenic animals and normal controls. Anatomy and embryology Mar;1999 199(3):239–248. [PubMed: 10068090]

29. Halloran BP, Ferguson VL, Simske SJ, Burghardt A, Venton LL, Majumdar S. Changes in bone structure and mass with advancing age in the male C57BL/6J mouse. J Bone Miner Res Jun;2002 17 (6):1044–1050. [PubMed: 12054159]

30. Pugener LA, Maglia AM. Skeletal morphogenesis of the vertebral column of the miniature hylid frog Acris crepitans, with comments on anomalies. Journal of morphology. Oct 22;2008

31. Rubin C, Turner AS, Muller R, Mittra E, McLeod K, Lin W, Qin YX. Quantity and quality of trabecular bone in the femur are enhanced by a strongly anabolic, noninvasive mechanical intervention. J Bone Miner Res Feb;2002 17(2):349–357. [PubMed: 11811566]

32. Paulus MJ, Gleason SS, Kennel SJ, Hunsicker PR, Johnson DK. High resolution X-ray computed tomography: an emerging tool for small animal cancer research. Neoplasia (New York, N.Y Jan-Apr;2000 2(12):62–70.

33. Pickhardt PJ, Halberg RB, Taylor AJ, Durkee BY, Fine J, Lee FT Jr. Weichert JP. Microcomputed tomography colonography for polyp detection in an in vivo mouse tumor model. Proceedings of the National Academy of Sciences of the United States of America Mar 1;2005 102(9):3419–3422. [PubMed: 15728368]

34. Marxen M, Thornton MM, Chiarot CB, Klement G, Koprivnikar J, Sled JG, Henkelman RM. MicroCT scanner performance and considerations for vascular specimen imaging. Medical physics Feb;2004 31(2):305–313. [PubMed: 15000616]
35. Jensen MM, Jorgensen JT, Binderup T, Kjaer A. Tumor volume in subcutaneous mouse xenografts measured by microCT is more accurate and reproducible than determined by 18F-FDG-microPET or external caliper. BMC medical imaging 2008;8:16. [PubMed: 18925932]
36. Kennel SJ, Davis IA, Branning J, Pan H, Kabalka GW, Paulus MJ. High resolution computed tomography and MRI for monitoring lung tumor growth in mice undergoing radioimmunotherapy: correlation with histology. Medical physics May;2000 27(5):1101–1107. [PubMed: 10841415]
37. Gruber HE, Ashraf N, Kilburn J, Williams C, Norton HJ, Gordon BE, Hanley EN Jr. Vertebral endplate architecture and vascularization: application of micro-computerized tomography, a vascular tracer, and immunocytochemistry in analyses of disc degeneration in the aging sand rat. Spine Dec 1;2005 30(23):2593–2600. [PubMed: 16319744]
38. Wirkner CS, Prendini L. Comparative morphology of the hemolymph vascular system in scorpions--a survey using corrosion casting, MicroCT, and 3D-reconstruction. Journal of morphology May;2007 268(5):401–413. [PubMed: 17372915]
39. Clauss SB, Walker DL, Kirby ML, Schimel D, Lo CW. Patterning of coronary arteries in wildtype and connexin43 knockout mice. Dev Dyn Oct;2006 235(10):2786–2794. [PubMed: 16802337]
40. Widmann G, Riedl A, Schoepf D, Glodny B, Peer S, Gruber H. State-of-the-art HR-US imaging findings of the most frequent musculoskeletal soft-tissue tumors. Skeletal radiology. Oct 10;2008
41. Cheung AM, Brown AS, Cucevic V, Roy M, Needles A, Yang V, Hicklin DJ, Kerbel RS, Foster FS. Detecting vascular changes in tumour xenografts using micro-ultrasound and micro-ct following treatment with VEGFR-2 blocking antibodies. Ultrasound in medicine & biology Aug;2007 33(8): 1259–1268. [PubMed: 17467156]
42. Flais S, Lassau N, Leclere J. Tumor vascularization: contribution of Doppler ultrasonography. Journal de radiologie 1996;77(12):1207–1212. [PubMed: 9033880]
43. Kaushik S, Miller TT, Nazarian LN, Foster WC. Spectral Doppler sonography of musculoskeletal soft tissue masses. J Ultrasound Med Dec;2003 22(12):1333–1336. [PubMed: 14682420]
44. Schroeder RJ, Hauff P, Bartels T, Vogel K, Jeschke J, Hidajat N, Maeurer J. Tumor vascularization in experimental melanomas: correlation between unenhanced and contrast enhanced power Doppler imaging and histological grading. Ultrasound in medicine & biology Jun;2001 27(6):761–771. [PubMed: 11516536]
45. Calliada F, Campani R, Bottinelli O, Bozzini A, Sommaruga MG. Ultrasound contrast agents: basic principles. European journal of radiology May;1998 27(Suppl 2):S157–160. [PubMed: 9652516]
46. Feleppa EJ, Alam SK, Deng CX. Emerging ultrasound technologies for early markers of disease. Disease markers 2002;18(56):249–268. [PubMed: 14646040]
47. McQuade P, Knight LC, Welch MJ. Evaluation of 64Cu- and 125I-radiolabeled bitistatin as potential agents for targeting alpha v beta 3 integrins in tumor angiogenesis. Bioconjugate chemistry Sep-Oct; 2004 15(5):988–996. [PubMed: 15366951]
48. Wang H, Cai W, Chen K, Li ZB, Kashefi A, He L, Chen X. A new PET tracer specific for vascular endothelial growth factor receptor 2. European journal of nuclear medicine and molecular imaging Dec;2007 34(12):2001–2010. [PubMed: 17694307]
49. Wu Y, Zhang X, Xiong Z, Cheng Z, Fisher DR, Liu S, Gambhir SS, Chen X. microPET imaging of glioma integrin {alpha}v{beta}3 expression using (64)Cu-labeled tetrameric RGD peptide. J Nucl Med Oct;2005 46(10):1707–1718. [PubMed: 16204722]
50. Cherry SR, Shaol Y, Silverman RW, Meadorsl K, Siegell S, Chatziioannoul A, Young JW, Jones WF, Moyers JC, Newport D, Boutefnouchetl A, Farquharl TH, Andreaco M, Paulus MJ, Binkley DM, Nutt R, Phelps ME. MicroPET: A High Resolution PET Scanner for Imaging Small Animals. IEEE TRANSACTIONS ON NUCLEAR SCIENCE 1997;44(3):1161–1166.
51. Chen JC, Chang SM, Hsu FY, Wang HE, Liu RS. MicroPET-based pharmacokinetic analysis of the radiolabeled boron compound [18F]FBPA-F in rats with F98 glioma. Appl Radiat Isot Nov;2004 61 (5):887–891. [PubMed: 15308163]
52. Chen X, Park R, Hou Y, Khankaldyyan V, Gonzales-Gomez I, Tohme M, Bading JR, Laug WE, Conti PS. MicroPET imaging of brain tumor angiogenesis with 18F-labeled PEGylated RGD peptide.

European journal of nuclear medicine and molecular imaging Aug;2004 31(8):1081–1089. [PubMed: 15118844]

53. Wu AM, Yazaki PJ, Tsai S, Nguyen K, Anderson AL, McCarthy DW, Welch MJ, Shively JE, Williams LE, Raubitschek AA, Wong JY, Toyokuni T, Phelps ME, Gambhir SS. High-resolution microPET imaging of carcinoembryonic antigen-positive xenografts by using a copper-64-labeled engineered antibody fragment. Proceedings of the National Academy of Sciences of the United States of America Jul 18;2000 97(15):8495–8500. [PubMed: 10880576]
54. Zhang X, Xiong Z, Wu Y, Cai W, Tseng JR, Gambhir SS, Chen X. Quantitative PET imaging of tumor integrin alphavbeta3 expression with 18F-FRGD2. J Nucl Med Jan;2006 47(1):113–121. [PubMed: 16391195]
55. Wu Y, Zhong Z, Huber J, Bassi R, Finnerty B, Corcoran E, Li H, Navarro E, Balderes P, Jimenez X, Koo H, Mangalampalli VR, Ludwig DL, Tonra JR, Hicklin DJ. Anti-vascular endothelial growth factor receptor-1 antagonist antibody as a therapeutic agent for cancer. Clin Cancer Res Nov 1;2006 12(21):6573–6584. [PubMed: 17085673]
56. Zhu Z, Hattori K, Zhang H, Jimenez X, Ludwig DL, Dias S, Kussie P, Koo H, Kim HJ, Lu D, Liu M, Tejada R, Friedrich M, Bohlen P, Witte L, Rafii S. Inhibition of human leukemia in an animal model with human antibodies directed against vascular endothelial growth factor receptor 2. Correlation between antibody affinity and biological activity. Leukemia Mar;2003 17(3):604–611. [PubMed: 12646950]
57. Zhu Z, Rockwell P, Lu D, Kotanides H, Pytowski B, Hicklin DJ, Bohlen P, Witte L. Inhibition of vascular endothelial growth factor-induced receptor activation with anti-kinase insert domain-containing receptor single-chain antibodies from a phage display library. Cancer research Aug 1;1998 58(15):3209–3214. [PubMed: 9699643]
58. Delbaldo C, Raymond E, Vera K, Hammershaimb L, Kaucic K, Lozahic S, Marty M, Faivre S. Phase I and pharmacokinetic study of etaracizumab (Abegrin), a humanized monoclonal antibody against alphavbeta3 integrin receptor, in patients with advanced solid tumors. Investigational new drugs Feb; 2008 26(1):35–43. [PubMed: 17876527]
59. Gutheil JC, Campbell TN, Pierce PR, Watkins JD, Huse WD, Bodkin DJ, Cheresh DA. Targeted antiangiogenic therapy for cancer using Vitaxin: a humanized monoclonal antibody to the integrin alphavbeta3. Clin Cancer Res Aug;2000 6(8):3056–3061. [PubMed: 10955784]
60. McNeel DG, Eickhoff J, Lee FT, King DM, Alberti D, Thomas JP, Friedl A, Kolesar J, Marnocha R, Volkman J, Zhang J, Hammershaimb L, Zwiebel JA, Wilding G. Phase I trial of a monoclonal antibody specific for alphavbeta3 integrin (MEDI-522) in patients with advanced malignancies, including an assessment of effect on tumor perfusion. Clin Cancer Res Nov 1;2005 11(21):7851–7860. [PubMed: 16278408]
61. Cai W, Wu Y, Chen K, Cao Q, Tice DA, Chen X. In vitro and in vivo characterization of 64Cu-labeled Abegrin, a humanized monoclonal antibody against integrin alpha v beta 3. Cancer research Oct 1;2006 66(19):9673–9681. [PubMed: 17018625]
62. Zimmermann K, Grunberg J, Honer M, Ametamey S, Schubiger PA, Novak-Hofer I. Targeting of renal carcinoma with 67/64Cu-labeled anti-L1-CAM antibody chCE7: selection of copper ligands and PET imaging. Nuclear medicine and biology May;2003 30(4):417–427. [PubMed: 12767399]
63. Logan TF, Jadali F, Egorin MJ, Mintun M, Sashin D, Gooding WE, Choi Y, Bishop H, Trump DL, Gardner D, Kirkwood J, Vlock D, Johnson C. Decreased tumor blood flow as measured by positron emission tomography in cancer patients treated with interleukin-1 and carboplatin on a phase I trial. Cancer chemotherapy and pharmacology Dec;2002 50(6):433–444. [PubMed: 12451469]
64. Schmidt KC, Turkheimer FE. Kinetic modeling in positron emission tomography. Q J Nucl Med Mar; 2002 46(1):70–85. [PubMed: 12072847]
65. Backer MV, Levashova Z, Patel V, Jehning BT, Claffey K, Blankenberg FG, Backer JM. Molecular imaging of VEGF receptors in angiogenic vasculature with single-chain VEGF-based probes. Nature medicine Apr;2007 13(4):504–509.
66. Guo L, Burke P, Lo SH, Gandour-Edwards R, Lau D. Quantitative analysis of angiogenesis using confocal laser scanning microscopy. Angiogenesis 2001;4(3):187–191. [PubMed: 11911016]
67. Inai T, Mancuso M, Hashizume H, Baffert F, Haskell A, Baluk P, Hu-Lowe DD, Shalinsky DR, Thurston G, Yancopoulos GD, McDonald DM. Inhibition of vascular endothelial growth factor (VEGF) signaling in cancer causes loss of endothelial fenestrations, regression of tumor vessels, and

appearance of basement membrane ghosts. The American journal of pathology Jul;2004 165(1):35–52. [PubMed: 15215160]

68. Hajnal, J.; Hill, D.; Hawkes, D. Medical Image Registration. CRC Press; 2001.
69. Zagorchev L, Goshtasby A. A Comparative Study of Transformation Functions for Nonrigid Image Registration. IEEE Transactions on image processing 2006;15(3)
70. Zitova B, Flusser J. Image registration methods: a survey. Image and Vision Computing 2003;21:977–1000.
71. Goshtasby, A. 2D and 3D Image Registration: for Medical, Remote Sensing, and Industrial Applications. Wiley-Interscience; 2005.

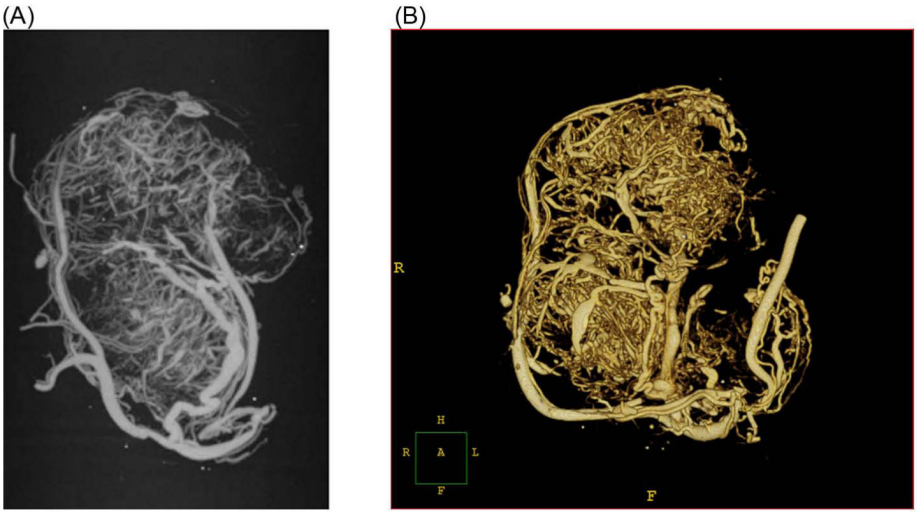

Figure 1. microCT imaged tumors

A MicroCT volume of a tumor harvested from the flank of an athymic mouse. The mouse was perfused with Microfil and imaged at 13 microns. The neo-vasculature of the tumor is shown as a maximum intensity projection (A), and a volumetric surface rendered in 3-D (B).

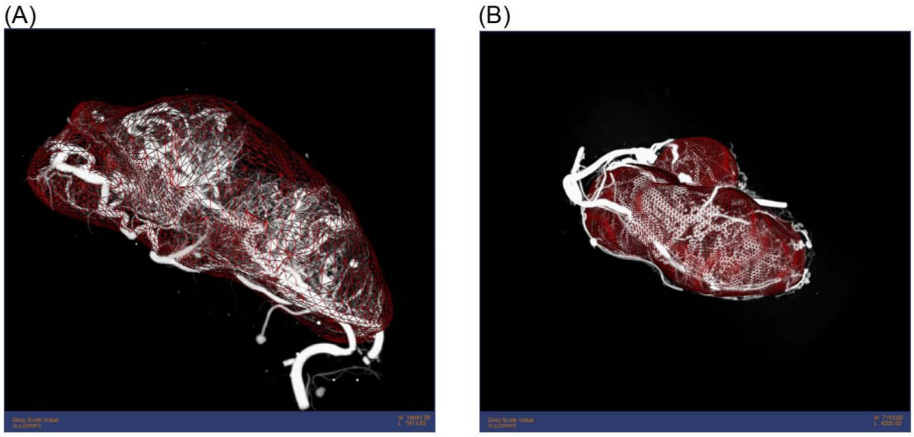

Figure 2. Three dimensional images of tumors

Three dimensional volume rendering showing the neo-vasculature and volume of a tumor harvested from the flank of a mouse treated with (A) saline and (B) rPAI-1_{23}. Note that the tumor treated with rPAI-1_{23} has much smaller volume as computed from the space enclosed by the triangulated mesh (red).

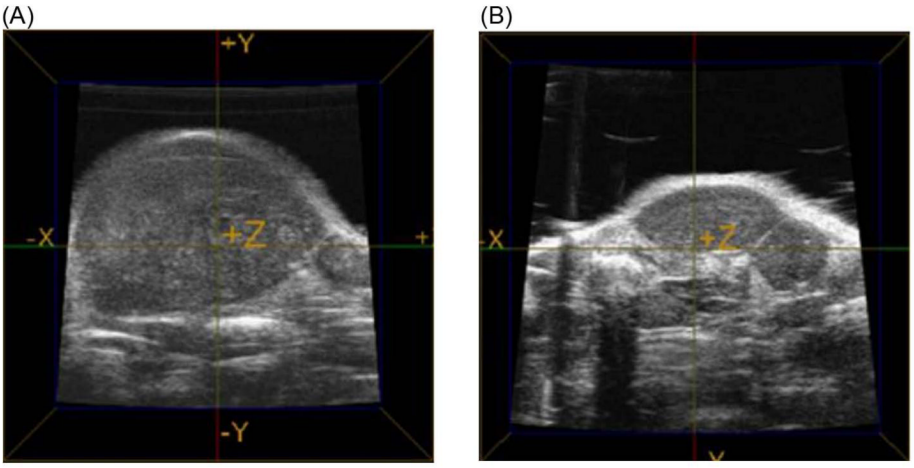

Figure 3. Ultrasound imaging of tumors

Slices from three dimensional ultrasound volumes showing the volume of a tumor harvested from the flank of a mouse treated with (A) saline or (B) rPAI-1_{23}.

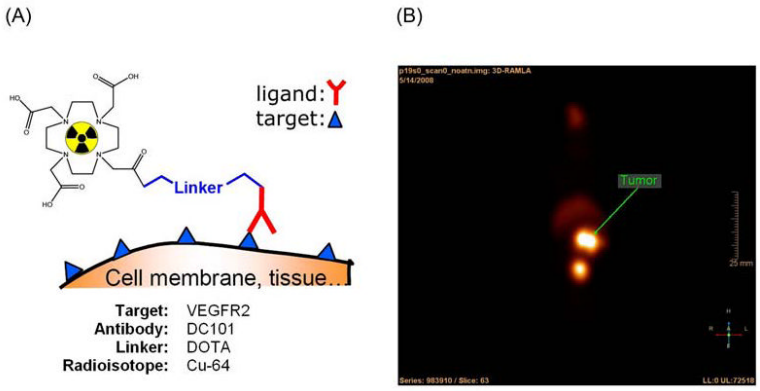

Figure 4. MicroPET imaging of antibody binding to vascular target

(A) A scheme for targeted microPET imaging of angiogenic markers and (B) a slice from a microPET volume showing Cu-64 labeled antibodies bound to the vasculature of a tumor implanted in a mouse.

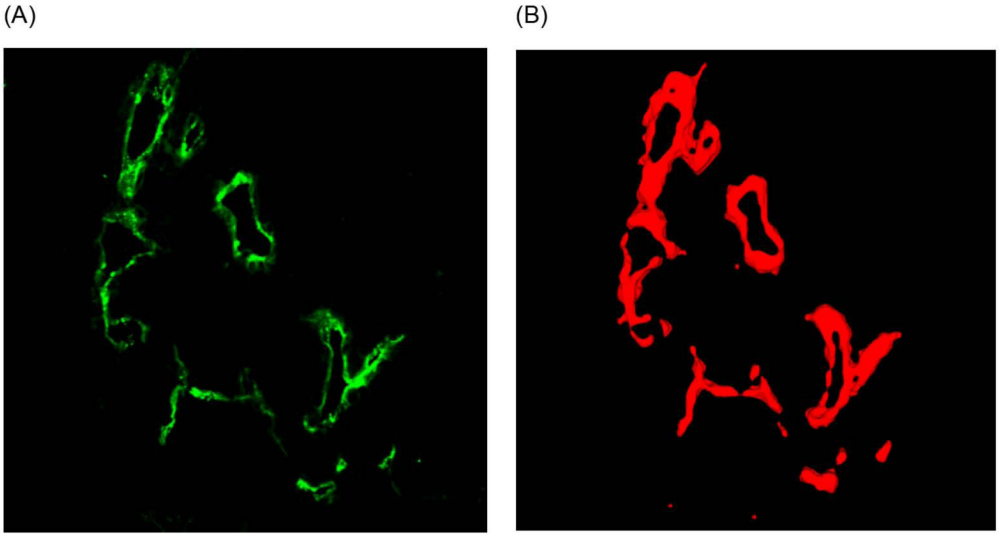

Figure 5. Confocal imaging of tumor blood vessels

A) A slice from a z-stack of a confocal image of a tumor stained for lectin, which is expressed on the surface of endothelial cells, and B) volumetric segmentation of the data that allows for quantification of the volume and density of the imaged target.

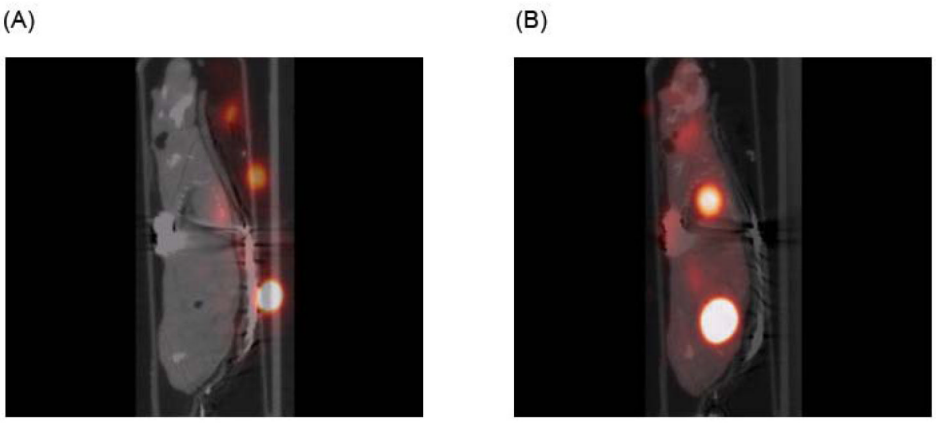

Figure 6. Registration of microPET and microCT images

A sagittal view of micro PET/CT volumes before (left) and after registration (right). Functional activity from microPET can be overlaid with structural information from microCT for more detailed analysis and validation of results.